

# INTERNATIONAL SOCIETY FOR SOIL MECHANICS AND GEOTECHNICAL ENGINEERING



*This paper was downloaded from the Online Library of the International Society for Soil Mechanics and Geotechnical Engineering (ISSMGE). The library is available here:*

<https://www.issmge.org/publications/online-library>

*This is an open-access database that archives thousands of papers published under the Auspices of the ISSMGE and maintained by the Innovation and Development Committee of ISSMGE.*

# Influence of the Variation of the Intermediate Principal Stress on the Mechanical Properties of Normally Consolidated Clays

Influence de la variation de l'effort principal intermédiaire sur les propriétés mécaniques des argiles normalement consolidées

T. SHIBATA, DR.ENG., *Assistant Professor, Disaster Prevention Research Institute, Kyoto University, Kyoto, Japan*  
D. KARUBE, *Assistant, Kyoto University, Kyoto, Japan*

## SUMMARY

The results of experimental study of the deformations, pore pressures, and shearing strengths of normally consolidated clays in three-dimensional stress space are presented. Tests by means of equipment which permits independent control of the three principal stresses on a specimen, and triaxial compression and extension tests were performed.

The relative value of the intermediate principal stress affects to some degree the deformations, pore pressures, and the shearing strengths expressed in terms of effective stress. The failure strain decreases with increasing value of the difference between the intermediate principal stress and minor principal stress. Behaviour of pore pressures can be adequately expressed by Henkel's equation, generalized by introducing stress invariants, and a critical value of the octahedral shear stress exists, below which dilatancy is zero. The Mohr-Coulomb failure surface represents the lower limits of the shearing strength, and the actual failure surface for clays is a curved one which circumscribes the Mohr-Coulomb hexagon.

## SOMMAIRE

Les résultats d'études expérimentales de déformations, pressions interstitielles et résistance au cisaillement d'argiles normalement consolidées dans l'espace sont présentés. Des essais sur argile utilisant l'équipement qui permet le contrôle indépendant des trois tensions principales sur un spécimen ainsi que des essais de compression triaxiale et d'extension ont été exécutés.

La valeur relative de la tension principale intermédiaire affecte les déformations, pressions interstitielles et résistances au cisaillement exprimées par les tensions efficaces jusqu'à un certain degré. La déformation à la rupture diminue avec l'augmentation de la valeur de la différence entre la tension principale intermédiaire et la tension principale mineure. L'action de la pression interstitielle peut être définie adéquatement par l'équation d'Henkel, généralisée par l'introduction de la tension invariable, et la valeur critique de l'effort de cisaillement octaèdre existe, lorsque la dilatabilité est nulle. La surface de rupture de Mohr-Coulomb représente la limite inférieure de la résistance au cisaillement et la surface véritable de rupture pour l'argile est la surface courbe qui circonscrit l'hexagone de Mohr-Coulomb.

THE MOHR-COULOMB FAILURE CRITERIA implicitly assume that the strength is independent of the intermediate principal stress. The influence of the variation of the intermediate principal stress on the shearing strength of clays was studied by Habib (1953), Haythornthwaite (1960), and Wu, *et al.* (1963). Habib performed torsional cylinder tests and Haythornthwaite torsional hollow cylinder tests. Both found considerable departures from the Mohr-Coulomb criteria expressed in terms of total stress. Wu, *et al.* performed hollow cylinder triaxial tests and concluded that the Mohr-Coulomb criteria expressed in terms of the Hvorslev strength parameters were valid for clays.

In this paper, equipment which permits independent control of the three principal stresses of  $\sigma_1$ ,  $\sigma_2$ , and  $\sigma_3$  on a rectangular cross-section specimen is described, and the results of conventional triaxial tests and tests for intermediate values of the second principal stress are presented.

## EQUIPMENT AND EXPERIMENTAL PROCEDURE

### Specimens

Remoulded samples of Osaka alluvial clay were reconsolidated in a large consolidometer having a diameter of 25 cm under a normal pressure of 0.45 kg/sq.cm. Test specimens 6 cm in length, 2 cm in thickness, and 3.5 cm in

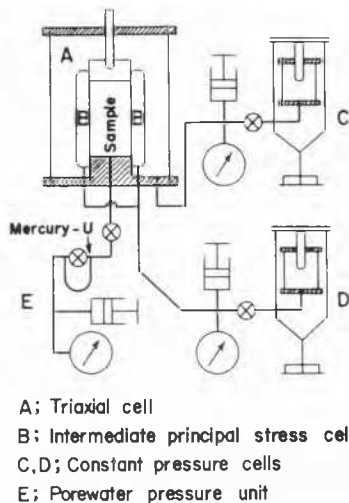
width were trimmed from a block of reconsolidated clay, and were subsequently consolidated in triaxial cells under all-round pressures ranging from 0.5 to 3.0 kg/sq.cm. before shear tests were carried out. Some properties of the clay are:  $w_1$ , 69 per cent,  $w_1$ , 20 per cent,  $I_p$ , 49 per cent, and activity, 2.0.

### Equipment

The schematic layout of apparatus used to obtain variation of the intermediate principal stress,  $\sigma_2$ , between the values of the major and minor principal stresses,  $\sigma_1$  and  $\sigma_3$ , is shown in Fig. 1. The major components are: the triaxial cell A, the intermediate principal stress cell B, the constant pressure cells C and D, and the pore-water-pressure unit E.

Details of the intermediate principal stress cell which consists of aluminum plates, membrane cushions, double membranes with silicone grease in between, and counterbalances are shown in Fig. 2. The double membranes and counterbalances are used to eliminate friction between the membrane cushions and the specimen. The space inside the membrane cushions is filled with water and connected to constant pressure cell D (Fig. 1).

The constant pressure cells C and D (Fig. 1) regulate the principal stresses,  $\sigma_3$  and  $\sigma_2$ , applied on the specimen. These applied stresses on the rectangular cross-section specimen



### Compression and Extension Tests

Rectangular cross-section specimens were subjected to undrained compression and extension tests with pore-water-pressure measurements. The same rate of strain, 0.01 per cent per min, was used in both the compression and the extension tests. In the compression tests,  $\sigma_1 > \sigma_2 = \sigma_3$ , failure was brought about by increasing the axial stress, keeping the triaxial cell pressure constant. In the extension tests,  $\sigma_1 = \sigma_2 > \sigma_3$ , failure was produced by decreasing the axial stress, keeping the triaxial cell pressure constant.

### $\sigma_1 > \sigma_2 > \sigma_3$ Tests

The loading procedures used in the tests for intermediate values of the second principal stress,  $\sigma_1 > \sigma_2 > \sigma_3$ , are shown in Fig. 3b in a three-dimensional stress space. The specimens are first consolidated under an all-round pressure,  $\sigma_c$ , at the point a. After consolidation,  $\sigma_1$  and  $\sigma_2$  are increased simultaneously by a certain quantity over  $\sigma_3$  which is held constant. The loading path followed in this portion of the tests is shown by the line a-b, and the stress conditions are therefore similar to those of extension tests. The specimen is then loaded to failure by increasing  $\sigma_1$  while  $\sigma_2$  and  $\sigma_3$  remain constant as shown by the line b-c.

In the loading portions shown by the line a-b-c, the specimen is loaded in the undrained condition with pore-water-pressure measurements. The dimensions of specimens and strain rate are the same as those of the compression and extension tests.

are shown in Fig. 3a. Details of the constant-pressure and pore-water-pressure equipment have been given by Andresen and Simons (1960).

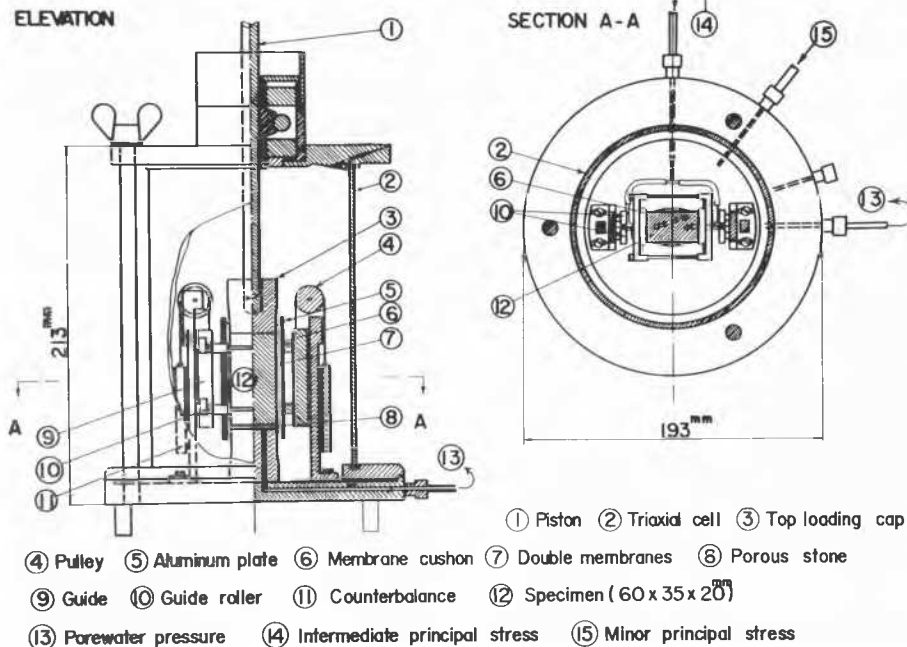


FIG. 2. Loading apparatus for intermediate principal stress.

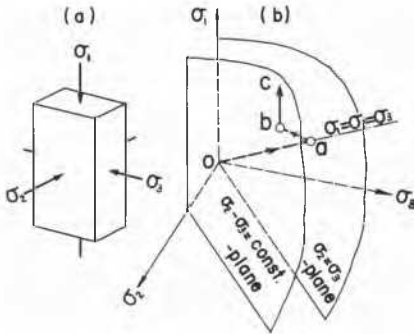


FIG. 3. (a) Applied stresses on the rectangular cross-section specimen. (b) Loading paths used in  $\sigma_1 > \sigma_2 > \sigma_3$  tests.

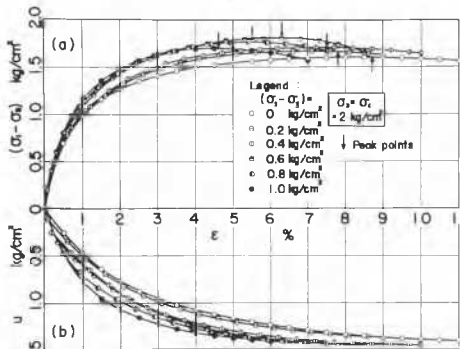


FIG. 4. (a) Relationship of principal stress difference ( $\sigma_1 - \sigma_3$ ) and major principal strain. (b) Relationship between pore water pressure and major principal strain.

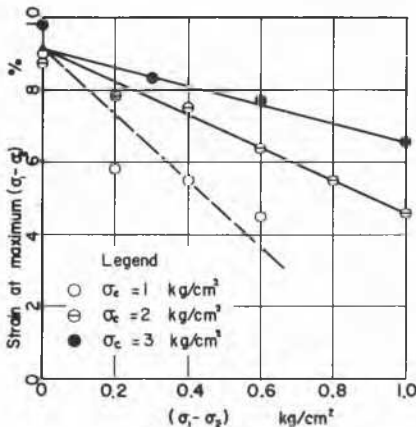


FIG. 5. Relationship of strain at maximum principal stress difference ( $\sigma_1 - \sigma_3$ ) and principal stress difference ( $\sigma_2 - \sigma_3$ ).

### Stress-Strain Relationship

Typical stress-strain and pore water pressure-strain curves for various values of the principal stress differences ( $\sigma_2 - \sigma_3$ ) are given in Fig. 4. The curves plotted in this figure were obtained from specimens consolidated at an all-round pressure of 2.0  $\text{kg/sq.cm}$ . Space limitations preclude presenting the curves of a similar type obtained from the specimens having other all-round consolidation pressures.

Fig. 4a and other stress-strain curves of similar type indicate that the shape of the stress-strain curve is influenced by the relative value of the intermediate principal stress, and that an increase in the value of principal stress difference ( $\sigma_2 - \sigma_3$ ) brings about a decrease in the value of strain at maximum principal stress difference ( $\sigma_1 - \sigma_3$ ). Moreover, as plotted in Fig. 5, the decrease in strain at maximum ( $\sigma_1 - \sigma_3$ ) is proportional to the value of ( $\sigma_2 - \sigma_3$ ), and a smaller strain is clearly obtained for the specimen consolidated under a lower all-round pressure.

### Pore Water Pressure

For saturated clays, the change in pore water pressures,  $\Delta u$ , due to changes in the three principal stresses of  $\Delta\sigma_1$ ,  $\Delta\sigma_2$ , and  $\Delta\sigma_3$ , is given as follows (Henkel, 1958):

$$\Delta u = \Delta\sigma_m + (D/C)\Delta\tau_{\text{oct}} \quad (1)$$

where

$$\Delta\sigma_m = \frac{1}{3}(\Delta\sigma_1 + \Delta\sigma_2 + \Delta\sigma_3)$$

$$\Delta\tau_{\text{oct}} = \frac{1}{3}\sqrt{(\Delta\sigma_1 - \Delta\sigma_2)^2 + (\Delta\sigma_2 - \Delta\sigma_3)^2 + (\Delta\sigma_3 - \Delta\sigma_1)^2}$$

and  $C$  = coefficient of compressibility,  $D$  = coefficient of dilatancy,  $\Delta\sigma_m$  = change in mean principal stress, and  $\Delta\tau_{\text{oct}}$  = change in octahedral shear stress.

Eq 1 may be written in the dimensionless form

$$(\Delta u - \Delta\sigma_m)/\sigma_m = (D/C)(\Delta\tau_{\text{oct}}/\sigma_m) \quad (2)$$

In Fig. 6 are plotted the values of  $(\Delta u - \Delta\sigma_m)/\sigma_m$  and  $\Delta\tau_{\text{oct}}/\sigma_m$  obtained from the triaxial compression and  $\sigma_1 > \sigma_2 > \sigma_3$  tests on specimens normally consolidated under 1.0, 2.0, and 3.0  $\text{kg/sq.cm}$ . The principal stress differences ( $\sigma_2 - \sigma_3$ ) in  $\sigma_1 > \sigma_2 > \sigma_3$  tests varied from 0.2 to 1.0  $\text{kg/sq.cm}$ .

Although a certain amount of scatter is inevitable in Fig. 6, it will be seen that there is a unique relationship

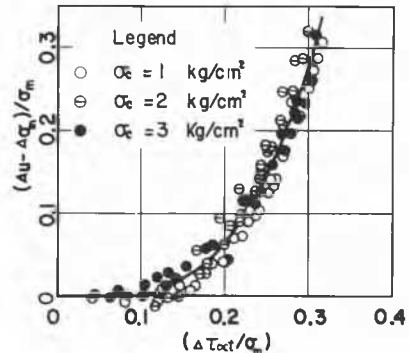


FIG. 6. Pore-water-pressure changes due to changes in the three principal stresses.

between the two quantities,  $(\Delta u - \Delta \sigma_m)/\sigma_m$  and  $\Delta \tau_{oct}/\Delta \sigma_m$ , irrespective of the relative value of the intermediate principal stress and the water content at the start of shear test. Moreover, it will be noted that a critical value of the change in octahedral shear stress exists, below which the coefficient of dilatancy  $D$  in Eq 2 is zero. Thus, the change in pore water pressure can be expressed as a function of  $\sigma_m$ ,  $\Delta \sigma_m$ , and  $\Delta \tau_{oct}$  by the equation

$$\left. \begin{aligned} \Delta \tau_{oct} < \Delta \tau_c; \Delta u = \Delta \sigma_m \\ \Delta \tau_{oct} > \Delta \tau_c; \Delta u = \Delta \sigma_m + \sigma_m f(\Delta \tau_{oct}/\sigma_m) \end{aligned} \right\} \quad (3)$$

where  $\Delta \tau_c$  = critical shear stress, below which dilatancy is zero.

### Stress Path and Strength

In Fig. 7 the stress paths followed in undrained compression, extension, and  $\sigma_1 > \sigma_2 > \sigma_3$  tests on normally consolidated clays are plotted in the plane of symmetry,  $\sigma'_2 = \sigma'_3$ . In addition, the failure envelopes for these tests are indicated.

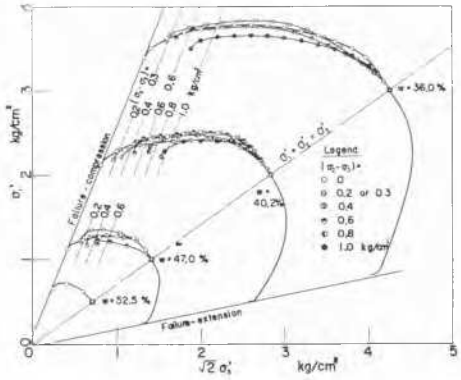


FIG. 7. Undrained stress paths for normally consolidated clays projected onto the plane of symmetry,  $\sigma'_2 = \sigma'_3$ .

As the actual points representing the stress conditions in  $\sigma_1 > \sigma_2 > \sigma_3$  tests lie in the plane of  $(\sigma_2 - \sigma_3) = \text{const.}$ , Fig. 3b, the stress paths followed in these tests are projected onto the plane of symmetry. The failure envelopes for  $\sigma_1 > \sigma_2 > \sigma_3$  tests, shown in Fig. 7 by the dashed lines, are drawn by assuming that the Mohr-Coulomb failure criteria are valid, and that parameters  $c'$  and  $\phi'$  are constant or independent of the value of the intermediate principal stress.

From Fig. 7, it will be seen that the shapes of the stress paths followed in the compression and  $\sigma_1 > \sigma_2 > \sigma_3$  tests are generally similar, and that the peak values of the effective stress ratio  $(\sigma'_1/\sigma'_3)$  for  $\sigma_1 > \sigma_2 > \sigma_3$  tests are greater than those for the conventional triaxial compression tests.

In Fig. 8 the results of compression, extension, and  $\sigma_1 > \sigma_2 > \sigma_3$  tests are shown in the plot of shear stress  $\frac{1}{2}(\sigma'_1 - \sigma'_3)$  versus normal stress  $\frac{1}{2}(\sigma'_1 + \sigma'_3)$ . There is no significant difference between the results of compression and extension tests, and the parameters  $c'$  and  $\phi'$  are 0.02 kg/sq.cm. and  $33.7^\circ$ . However, the strength obtained from  $\sigma_1 > \sigma_2 > \sigma_3$  tests differs somewhat from that obtained in conventional triaxial tests. The nature of these departures are examined by projecting the measured stresses at failure

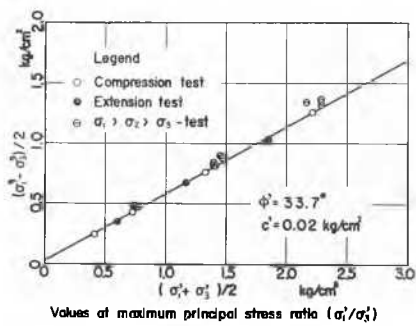


FIG. 8. Relationship between strength and effective normal stress; a comparison of the results of  $\sigma_1 > \sigma_2 > \sigma_3$  tests and conventional triaxial tests.

onto an octahedral plane, using the apex of the failure envelope as a centre of projection (Wu, *et al.*).

Fig. 9 shows a right section of the theoretical Mohr-Coulomb failure surface which is determined by the values of  $c' = 0.02$  kg/sq.cm. and  $\phi' = 33.7^\circ$  measured in the compression and extension tests. The results obtained from  $\sigma_1 > \sigma_2 > \sigma_3$  tests are also plotted as points. The actual failure surface for normally consolidated clays has a curved form, as shown in Fig. 9 by the dashed line, and the Mohr-Coulomb hexagon represents the inner limit of the failure surface of clays. Hence the difference is on the safe side if our estimates of factor of safety are based on conventional triaxial tests.

### CONCLUSIONS

A series of conventional consolidated-undrained triaxial tests and tests for intermediate values of the second principal stress were performed on normally consolidated clays. The main results obtained are as follows.

1. The shape of the stress-strain curve is influenced by the relative value of intermediate principal stress, and the axial strain at the maximum principal stress difference  $(\sigma_1 - \sigma_3)$  decreases with increasing value of the principal stress difference  $(\sigma_2 - \sigma_3)$ .

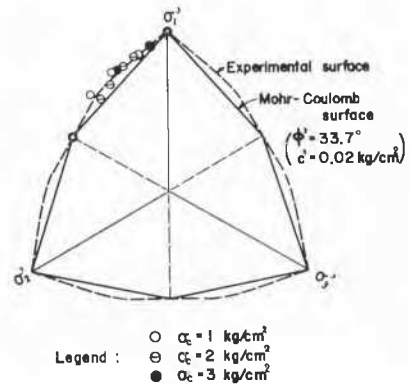


FIG. 9. Right section of experimental and Mohr-Coulomb failure surfaces.

2. The change in pore water pressure due to changes in the three principal stresses can be adequately expressed as a function of  $\sigma_m$ ,  $\Delta\sigma_m$ , and  $\Delta\sigma_{oct}$ , where  $\sigma_m$  is the mean principal stress and  $\tau_{oct}$  is the octahedral shear stress.

3. Close agreement is found in the values of  $\phi'$  for compression and extension tests, but slightly larger values of  $\phi'$  for intermediate stress conditions are obtained.

4. The Mohr-Coulomb failure surface represents the lower limits of shearing strength, and the actual failure surface for normally consolidated clays is a curved surface which circumscribes the Mohr-Coulomb hexagon.

#### ACKNOWLEDGMENT

The writers wish to acknowledge the aid and advice given by Professor S. Murayama of Kyoto University.

#### REFERENCES

- ANDRESEN, A., and N. E. SIMONS (1960). Norwegian triaxial equipment and technique, *Proc. Conference on Shear Strength of Cohesive Soils*, American Society of Civil Engineers, p. 659.
- HABIB, M. P. (1953). Influence of the variation of the intermediate principal stress on the shearing strength of soils, *Proc. Third International Conference on Soil Mechanics and Foundation Engineering*, Vol. 1, p. 131.
- HAYTHORNTHWAITTE, R. M. (1960). Stress and strain in soils. In *Plasticity*, p. 1958. New York, Pergamon Press, Inc.
- HENKEL, D. J. (1960). The shear strength of saturated remoulded clays, *Proc. Conference on Shear Strength of Cohesive Soils*, American Society of Civil Engineers, p. 533.
- WU, T. H., A. K. LOH, and L. E. MALVERN (1963). Study of failure envelope of soils, *Proc. American Society of Civil Engineers*, Vol. 89 (SM 1), p. 145.